

## Valproate-induced Encephalopathy: Assessment with MR Imaging and $^1\text{H}$ MR Spectroscopy

\*Sargon Ziyeh, †Thorsten Thiel, \*Joachim Spreer, \*Joachim Klisch, and \*Martin Schumacher

\*Section of Neuroradiology, Department of Neurosurgery, and †Section of Medical Physics, Department of Diagnostic Radiology, University Hospital, Freiburg, Germany

**Summary:** The anticonvulsant agent valproate (VPA) may cause hyperammonemic encephalopathy. Magnetic resonance imaging (MRI) and proton MR spectroscopic (MRS) findings in a patient with VPA-induced hyperammonemic encephalopathy are described. MRI showed a metabolic-toxic lesion pattern with bilateral  $T_2$ -hyperintense lesions in the cerebellar white matter and in the globus pallidus. MR spectroscopic find-

ings were indistinguishable from hepatic encephalopathy with severe depletion of myoinositol and choline and with glutamine excess. *N*-Acetylaspartate levels were moderately decreased. Quantitative MRS gave detailed insight into alterations of brain metabolism in VPA-induced encephalopathy. **Key Words:** Magnetic resonance imaging—Magnetic resonance spectroscopy—Valproate—Encephalopathy—Hyperammonemia.

Valproate (VPA) is an antiepileptic drug (AED) for the treatment of both generalized and partial seizures in children and adults. Besides this classic indication, the drug is increasingly used for therapy for bipolar and schizoaffective psychiatric disorders, neuropathic pain, and prophylactic treatment of migraine (1). Possible adverse effects are idiosyncratic fatal hepatotoxicity, teratogenicity, inhibited catabolism of other AEDs, such as phenobarbital (PB), and hyperammonemic encephalopathy without hepatic dysfunction (2,3).

We describe MR imaging (MRI) and proton MR spectroscopic ( $^1\text{H}$ -MRS) findings in a patient with VPA-induced hyperammonemia and encephalopathy without hepatic dysfunction. There is only one report on MRI findings in VPA encephalopathy in the literature (4).

### CASE REPORT

A 32-year-old patient had been treated with  $3 \times 500$ -mg VPA daily because of epileptic seizures since traumatic brain injury 6 years ago. The patient was admitted with vertigo, disturbance of concentration, slight gait ataxia, and asterixis. Laboratory findings and sonography excluded liver disease. Serum VPA level was within the therapeutic range (68 mg/L). Ammonia serum level was markedly elevated, with  $152 \mu\text{M}$  (normal range,

11–35), and gradually normalized after discontinuation of VPA. EEG showed generalized slowing of background activity characterized by slow alpha and theta activity. In addition, continuous theta and rare delta waves were visible bilaterally over frontal and fronto-basal regions. Within 1 month, these findings resolved, with improvement of clinical symptoms and decreasing  $\text{NH}_3$  serum levels.

MRI and  $^1\text{H}$ -MRS were performed on a 2-T whole body system (Bruker MEDSPEC S200) by using a quadrature head coil. Transversal  $T_{1w}$  spin-echo and transverse and coronal  $T_{2w}$  RARE sequences of the whole brain were acquired. For  $^1\text{H}$ -MRS we used a short echo time PRESS sequence (TR 1,500, TE 30, 256 averages). Eight-milliliter voxels were placed in the occipital lobe covering predominantly gray matter and in the left parietal lobe including mainly white matter.

For quantification of the metabolite concentrations, the signal from an external water reference was measured, omitting the water suppression with otherwise identical acquisition parameters (eight averages). Spectral analysis was performed with the LCModel algorithm (5). The program uses in vitro spectra of the expected metabolites as model functions. The concentrations were compared with results from a group of 25 normal control subjects.

### RESULTS

MRI depicted old contusion defects in the basal frontal lobes.  $T_{2w}$  images showed prominent bilateral symmetric

Accepted March 10, 2002.

Address correspondence and reprint requests to Dr. S. Ziyeh at Section of Neuroradiology, Department of Neurosurgery, University Hospital, Breisacherstr. 64, D-79106 Freiburg, Germany. E-mail: ziyeh@nz.ukl.uni-freiburg.de

hyperintense signal of the cerebellar white matter. These changes abutted the dentate nucleus from laterally (Fig. 1). Bilateral  $T_2$  hyperintense lesions in the globus pallidus were shown in addition (Fig. 2).  $^1\text{H}$ -MRS showed marked abnormalities of the choline (Cho), myoinositol (MyI), and glutamate/glutamine (Glu/Gln) resonances (Fig. 3; Table 1).

Cho signal was diminished by ~50%. Absolute concentrations were 0.6 mmol/kg wet weight (mmol/kg ww) in both locations (normal value, 1.4). MyI was markedly depleted, with a concentration of 0.9 mmol/kg ww in

occipital gray matter (normal value, 4.4). MyI was undetectable in the parietal mainly white-matter voxel.

$^1\text{H}$ -MRS showed prominent signal amplitudes at 3.75 and between 2.1 and 2.5 ppm, corresponding to the  $\alpha$ - and the  $\beta/\gamma$  protons of Glu and Gln, respectively (6).

At the time the patient was examined, we were not able to establish normal values for Glu and Gln for technical reasons. In comparison with results from the literature (7), Gln concentrations were elevated about fourfold (occipital) to sevenfold (parietal) above the mean normal value. Glu concentrations were decreased by ~30% in

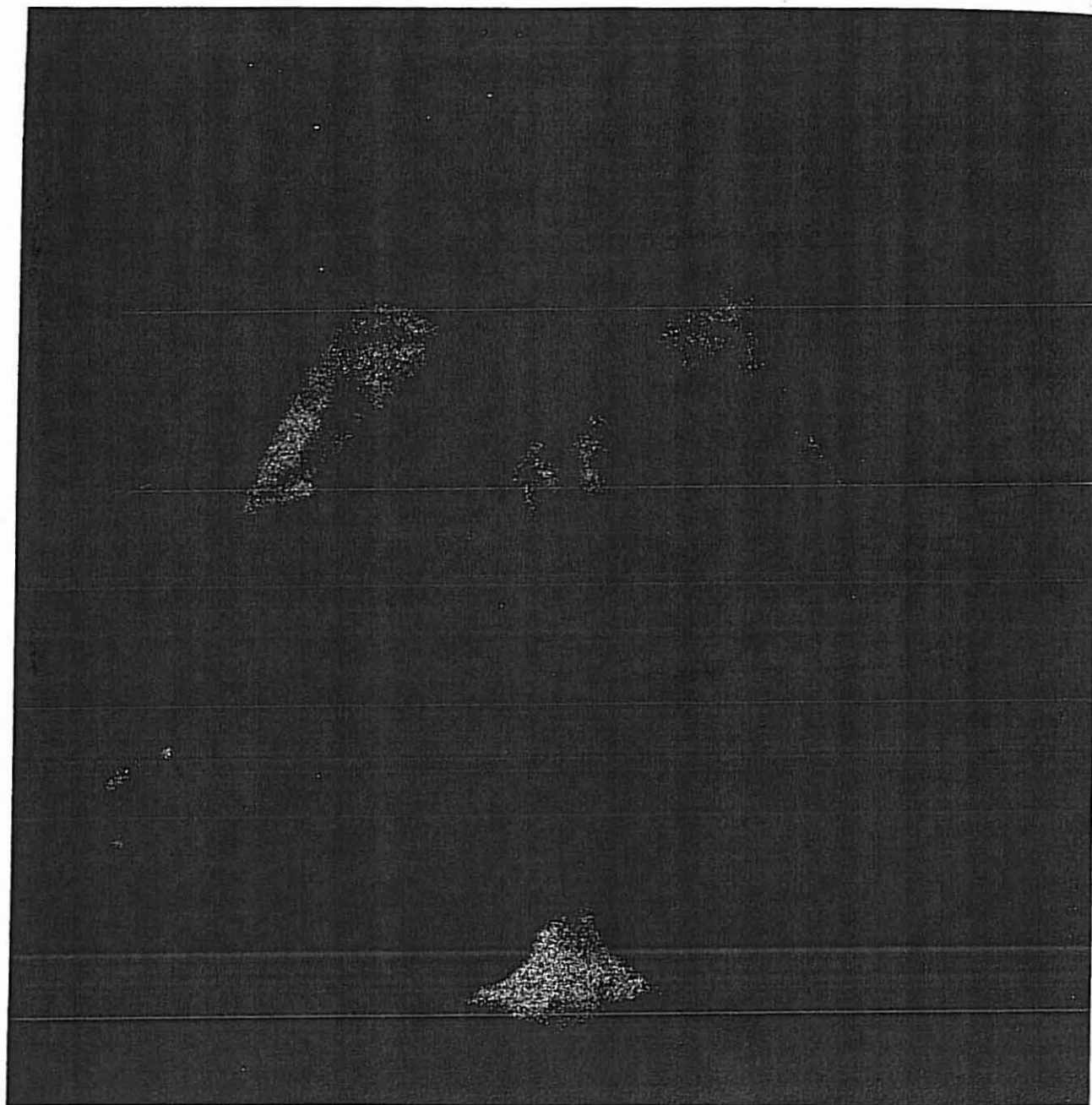


FIG. 1. Coronal  $T_2$  weighted magnetic resonance image showing prominent cerebellar white matter hyperintensities.

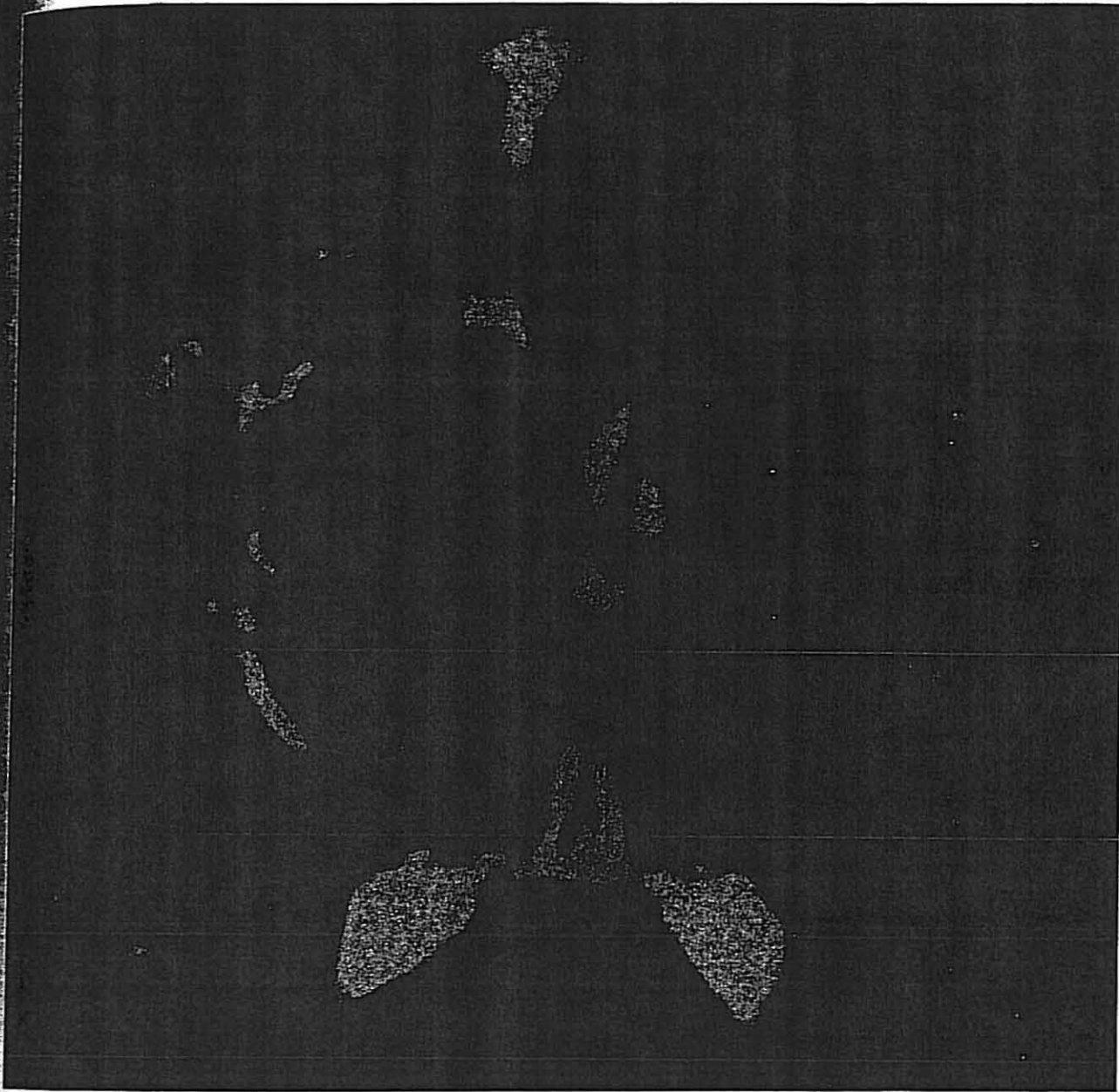


FIG. 2. Transverse  $T_{2w}$  magnetic resonance image. The bifrontal contusion defects extend to this level on the right side only. Relatively inconspicuous hyperintense lesions in the globus pallidus.

both locations. Glu + Gln ("Glx") was twice the mean normal level.

The LCModel algorithm determined *N*-acetylaspartate (NAA) concentrations of 7.3 (occipital) and 7.1 (parietal) mmol/kg ww. These values indicated a 30% reduction of NAA in comparison with that of normal control subjects.

#### DISCUSSION

VPA reduces hepatic citrullinogenesis through inhibition of hepatic carbamyl phosphate synthetase activity, therefore acting as an urea cycle inhibitor (8). Conse-

quently, patients with genetic defects of urea cycle enzymes are prone to VPA-induced hyperammonemia with encephalopathy. Undetected heterozygote and atypical late-onset cases may develop severe hyperammonemia with VPA administration (9,10).

However, in the majority of patients with VPA encephalopathy, enzymatic abnormalities are absent. In these patients, VPA-mediated inhibition of ammonia elimination through the hepatic urea cycle seems to become relevant with high nutritional amino acid load.

Patients with VPA-induced hyperammonemia are seen with confusion, lethargy, coma, ataxia, and asterixis. Se-

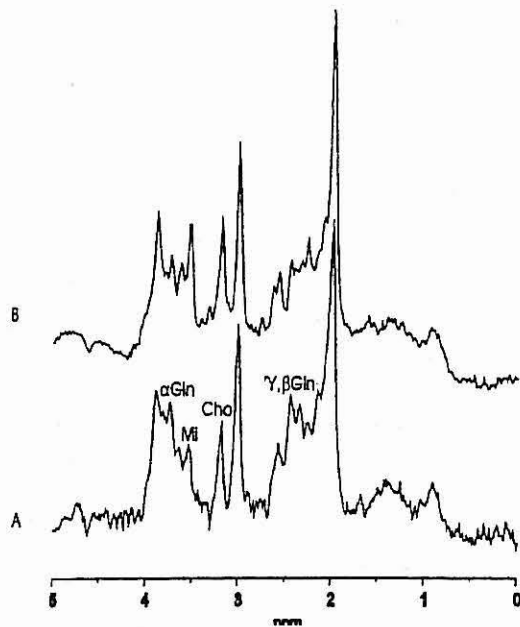


FIG. 3. Occipital magnetic resonance spectrum predominantly covering gray matter in valproate encephalopathy (A) compared with a normal control spectrum (B). Diminished signal amplitudes of choline and myoinositol. Elevated signals corresponding to  $\alpha$  and  $\beta/\gamma$  protons of glutamate and glutamine.

rum ammonia levels are elevated, usually at least about fourfold of the upper normal level. In contrast to hepatic encephalopathy—another hyperammonemic encephalopathy, with similar central nervous system symptoms—laboratory, imaging, or histopathologic signs of hepatic damage are lacking.

Baganz and Dross (4) described MRI findings in a patient with VPA encephalopathy. Extensive cortical brain areas with increased  $T_2$  signal were demonstrated in frontal, temporal, and insular locations. These signal changes were reversible, and mild atrophy of the affected cortex was noted on 1-year follow-up.

In contrast, our patient did not show cortical changes, apart from old frontobasal contusion defects. We found bilateral abnormal  $T_2$ -hyperintense signal in the globus pallidus and in cerebellar white matter. It is possible that differing serum ammonia levels result in a different pattern of brain injury. In the patient of Baganz et al. (4),

serum ammonia peaked to a value 15-fold above the upper normal limit, and in our patient, only sixfold.

Bilateral basal ganglia lesions are common in toxic-metabolic encephalopathies. In addition, cerebellar white matter may be involved in several metabolic disorders (11). The MRI pattern in our patient was consequently compatible with a toxic-metabolic encephalopathy.

To our knowledge this is the first report on  $^1\text{H}$ -MRS findings in VPA encephalopathy in the literature. Pathologic MRS features of VPA encephalopathy were a significant decrease of Cho and MyI resonances and Gln excess. This MRS pattern has been described in other hyperammonemic encephalopathies like acute (12) and chronic (13) hepatic encephalopathy.

Because of the strong overlap of the resonances of Gln and Glu in the spectral domain, contributions from the two metabolites are difficult to differentiate at a magnetic field strength of 2 T. The corresponding peak areas are therefore commonly assigned as the sum of both components, "Glx." The time domain fitting algorithm LCModel is able to separate the signals of Glu and Gln with a high level of significance, and their concentrations can be determined quantitatively (7).

Our MRS results reflect pathobiochemical considerations of Glu/Gln metabolism during hyperammonemia. The excitatory neurotransmitter Glu, once released to synaptic space, undergoes astrocytic uptake and metabolism to Gln through glutamine synthetase (GS). This step consumes equimolar ammonia. Gln is transported into neurons and converted to Glu by the neuronal enzyme glutaminase. Hyperammonemia has been shown to stimulate GS and to inhibit glutaminase. This leads to an accumulation of Gln and a moderate but significant depletion of Glu, as alternative sources of Glu synthesis fail to replenish the Glu pool (14). However, the total amount of Glu + Gln increases in hyperammonemic encephalopathies, producing elevated "Glx" in MRS.

VPA encephalopathy simulates MRS findings of hepatic encephalopathy with regard to Cho and MyI depletion. Reduction of MyI reflects its role as an organic cerebral osmolyte compensating for osmotically active Gln excess (14). The mechanisms of Cho depletion are still to be elucidated (14).

TABLE 1. Results of  $^1\text{H}$ -MRS in patient with VPA encephalopathy compared with normal controls

Brain metabolite concentration in mmol/kg wet weight	NAA	Cho	Gln	Glu	Gli + Glu	Crea	MyI
Patient, occipital gray matter (GM)	7.3	0.74	16.2	6.5	22.7	5.6	0.9
Patient, parietal white matter (WM)	7.1	0.74	13.3	4.1	17.4	3.8	0
Normal controls, occipital GM (n = 25)	11.8 ± 1.1	1.6 ± 0.2	4.1 ± 1.3 <sup>a</sup>	8.8 ± 1.1 <sup>a</sup>	12.9 <sup>a</sup>	6.9 ± 0.8	4.4 ± 0.7
Normal controls, parietal WM (n = 24)	10.7 ± 0.7	2.05 ± 0.21	1.8 ± 1.2 <sup>a</sup>	5.8 ± 1.2 <sup>a</sup>	7.6 <sup>a</sup>	5.4 ± 0.5	5.1 ± 0.7

MRS, magnetic resonance spectroscopy; NAA, *N*-acetylaspartate; Cho, choline; Gln, glutamine; Glu, glutamate; Crea, creatinine; MyI, myoinositol.  
<sup>a</sup> Values from Pouwels P, et al. 1999 (7).

We found a 30% reduction of cerebral NAA concentrations in VPA encephalopathy. In the spectroscopic literature, NAA is assigned as a neuronal marker indicating viability and density of neuronal tissue. However, in our patient, MRI did not depict cerebral morphologic changes suggestive of neuronal loss. There is accumulating evidence for a role of NAA as a neuronal molecular water pump (15). We speculate that reduction of NAA resonances in VPA encephalopathy could indicate disturbance of osmotic homeostasis on a cellular level.

In conclusion, MRI findings of our patient with VPA-induced hyperammonemia are compatible with a toxic-metabolic encephalopathy. The results of <sup>1</sup>H-MRS reflect the effects of hyperammonemia on Glu/Gln metabolism and cerebral osmoregulation. <sup>1</sup>H-MRS offers the opportunity to monitor cerebral metabolic alterations related to VPA therapy.

#### REFERENCES

1. Löscher W. Valproate: a reappraisal of its pharmacodynamic properties and mechanisms of action. *Prog Neurobiol* 1999;58:31-59.
2. Coulter DL, Allen RJ. Secondary hyperammonemia: a possible mechanism for valproate encephalopathy. *Lancet* 1980;1:310-1.
3. Kulick SK, Kramer DA. Hyperammonemia secondary to valproic acid as a cause of lethargy in a postictal patient. *Ann Emerg Med* 1993;22:610-2.
4. Baganz MD, Dross PE. Valproic acid-induced hyperammonemic encephalopathy: MR appearance. *Am J Neuroradiol* 1994;15:1779-81.
5. Provencher SW. Estimation of metabolite concentrations from localized in vivo proton NMR spectra. *Magn Reson Med* 1993;30:672-9.
6. Ross BD. Biochemical considerations in 1H spectroscopy: glutamate and glutamine; myoinositol and related metabolites. *NMR Biomed* 1991;4:59-63.
7. Pouwels P, Brockmann K, Kruse B, et al. Regional age dependence of human brain metabolites from infancy to adulthood as detected by quantitative localized proton MRS. *Pediatr Res* 1999;46:474-85.
8. Marini AM, Zaret BS, Beckner RR. Hepatic and renal contributions to valproic acid-induced hyperammonemia. *Neurology* 1988;38:365-71.
9. Horiuchi M, Imamura Y, Nakamura N, et al. Carbamoylphosphate synthetase deficiency in an adult: deterioration due to administration of valproic acid. *J Inher Metab Dis* 1993;16:39-45.
10. Honeycutt D, Callahan K, Rutledge L, et al. Heterozygote ornithine transcarbamylase deficiency presenting as symptomatic hyperammonemia during initiation of valproate therapy. *Neurology* 1992;42:666-8.
11. Steinlin M, Blaser S, Boltshauser E. Cerebellar involvement in metabolic disorders: a pattern-recognition approach. *Neuroradiology* 1988;40:347-54.
12. McConnell JR, Antonson DL, Ong CS, et al. Proton spectroscopy of brain glutamine in acute liver failure. *Hepatology* 1995;22:67-94.
13. Kreis R, Farrow N, Ross BD. Localized AHNMR spectroscopy in patients with chronic hepatic encephalopathy: analysis of changes in cerebral glutamine, choline and inositols. *NMR Biomed* 1991;4:109-16.
14. Kanamori K, Bluml S, Ross B. Magnetic resonance spectroscopy in the study of hyperammonemia and hepatic encephalopathy. *Adv Exp Med Biol* 1997;420:185-94.
15. Baslow MH. Molecular water pumps and the aetiology of Canavan disease: a case of the sorcerer's apprentice. *J Inher Metab Dis* 1999;22:99-101.